Signatures of spin-preserving symmetries in two-dimensional hole gases

Tobias Dollinger,[1] Andreas Scholz,[1] Paul Wenk,[1] R. Winkler,[2] John Schliemann,[1] and Klaus Richter[1]

[1]*Institut für Theoretische Physik, Universität Regensburg, D-93040 Regensburg, Germany*
[2]*Department of Physics, Northern Illinois University, IL 60115 DeKalb, USA*
(Dated: April 29, 2013)

We investigate ramifications of the persistent spin helix symmetry in two-dimensional hole gases in the conductance of disordered mesoscopic systems. To this end we extend previous models by going beyond the axial approximation for III-V semiconductors. We identify for heavy-hole subbands an exact spin-preserving symmetry analogous to the electronic case by analyzing the crossover from weak anti-localization to weak localization and spin transmission as a function of extrinsic spin-orbit interaction strength.

Control over spin relaxation is essential to the operational capabilities of spin-based semiconductor devices [1, 2]. A major advance in this respect has been the identification of an SU(2) symmetry that confines spin evolution to a characteristic topology denoted "persistent spin helix" (PSH) and prevents spin relaxation [2, 3]. The latter could be identified by means of optical experiments [4, 5] in two-dimensional electronic systems with linear-in-momentum Bychkov-Rashba [6] and Dresselhaus [7] type spin-orbit interactions (SOIs) (here depending on the parameters α and β, respectively) of equal magnitude. As had already been suggested in Refs. [8, 9], this symmetry at $\alpha = \beta$ also becomes manifest in the weak localization (WL) feature in magnetoconductance traces of disordered materials with finite SOI, as opposed to weak antilocalization (WAL) mediated by spin relaxation [10]. Recent experiments confirmed theoretical predictions that the WL signature persists for n-doped systems even in the presence of nonnegligable intrinsic SOI that scales as k^3 [11–13].

The question naturally arises whether the phenomenon of suppressed spin relaxation also exists in p-doped conductors. Here we hence investigate the generalization of the PSH symmetry arguments in the context of structurally confined heavy-hole (HH) states in III-V semiconductors forming a two-dimensional hole gas (2DHG). In these materials the spin is subject to strong SOIs which typically enhances spin relaxation. This feature is mainly attributed to the carrier density dependence of the spin splitting, that has been investigated analytically by means of diagrammatic perturbation theory within the spherical approximation for one or more subbands [14]. Other works consider weak (anti-) localization in hole gases based on a semianalytical [15] as well as a semiclassical and numerical [16] treatment of 4×4 Luttinger-Kohn models [17]. Here we focus on strong confinement described by an effective 2×2 model of the HH ground state. Our treatment is not restricted to the spherical or axial approximations, which significantly widens the range of observable phenomena compared to prior models. The low dimensionality allows for

the identification of relevant symmetries that are used to deduce optimum parameter regimes for controlling spin relaxation. The structure of our model is given by the Hamiltonian

$$H = H_{\text{kin}}\sigma_0 + \mathbf{\Omega}_{\text{2DHG}} \cdot \boldsymbol{\sigma}, \tag{1}$$

where H_{kin} denotes the kinetic energy, σ_0 the identity matrix, $\boldsymbol{\sigma}$ the vector of Pauli matrices, and $\mathbf{\Omega}_{\text{2DHG}}$ the effective spin-orbit field coupling to the spin. In contrast to the corresponding expression $\mathbf{\Omega}_{\text{2DEG}}$ for electrons, where k-linear terms are dominant [9], to leading order $\mathbf{\Omega}_{\text{2DHG}}$ is characterized by a cubic momentum dependence. This is in agreement with existing 2DHG models and results from coupling of the HH to the light hole (LH) subbands [18, 19]. The result (1) is obtained via a perturbative expansion of the standard Luttinger-Kohn Hamiltonian [17] in the basis given by the subband edge states in growth direction along the [001] crystal axis [20]. Our model is adequate to describe systems in which the energy level closest to the HH ground state is the LH ground state of the quantum well. This applies to typical zinc-blende structure materials, as can be inferred from their material properties and calculated band structures given e.g. in Ref. [20]. In Eq. (1) $\boldsymbol{\sigma}$ represents the subspace spanned by the HH states of spin angular-momenta $\pm 3/2$ and the hole spin-orbit field is given by

$$\begin{aligned}
\mathbf{\Omega}_{\text{2DHG}} = {}& \beta_{\text{HH}}\mathbf{k} \\
& + \lambda_{\text{D}}\left\{-\bar{\gamma}k_{\text{F}}^2\mathbf{k} + \delta[k_x^3\hat{\mathbf{x}} + k_y^3\hat{\mathbf{y}} - 3k_xk_y(k_y\hat{\mathbf{x}} + k_x\hat{\mathbf{y}})]\right\} \\
& + \lambda_{\text{R}}\left\{\delta k_{\text{F}}^2(k_y\hat{\mathbf{x}} + k_x\hat{\mathbf{y}}) + \bar{\gamma}[-k_y^3\hat{\mathbf{x}} - k_x^3\hat{\mathbf{y}} + 3k_xk_y\mathbf{k}]\right\}
\end{aligned} \tag{2}$$

with the intrinsic Dresselhaus parameters

$$\beta_{\text{HH}} = -\sqrt{3}C_k\left(\frac{1}{2} - \frac{2\hbar^2\langle k_z^2\rangle\gamma_3}{m_0\Delta_{\text{HL}}}\right), \tag{3}$$

$$\lambda_{\text{D}} = \frac{\sqrt{3}\hbar^2}{2m_0\Delta_{\text{HL}}}\left[C_k + \sqrt{3}b_{41}^{8v8v}\langle k_z^2\rangle\right], \tag{4}$$

the structural, electrical field $\langle E_z\rangle$ dependent Bychkov-

Rashba parameter,

$$\lambda_{\mathrm{R}} = \frac{3\hbar^2}{2m_0\Delta_{\mathrm{HL}}} \langle E_z \rangle r_{41}^{8v8v}, \tag{5}$$

and the Luttinger parameters $\bar{\gamma} = (\gamma_3 + \gamma_2)/2$ and $\delta = (\gamma_3 - \gamma_2)/2$ as in Ref. [21]. We denote the material constants C_k, r_{41}^{8v8v} and b_{41}^{8v8v} consistent with Ref. [20]. By going beyond the axially symmetric situation, $\delta = 0$, the above expression is a generalization to previous models [18, 19, 22]. This allows for the description of a broader range of materials and to avoid neglecting anisotropies that are of importance, for instance, in the plasmon spectra of HH systems [23]. Vertical confinement is modeled by a potential well with perpendicular wavenumber $\langle k_z^2 \rangle$ that displays a splitting $\Delta_{\mathrm{HL}} = 2\gamma_2\hbar^2 \langle k_z^2 \rangle /m_0$ between HH and LH-bands. For further analysis the terms proportional to the small parameter C_k are neglected in Eqs. (3,4), since for a narrow confinement they are dominated by the terms proportional to $b_{41}^{8v8v} \langle k_z^2 \rangle$ in realistic materials, as shown in Table 6.3 in Ref. [20].

Furthermore, the linear Dresselhaus term (3) effectively rescales the axially symmetric part of the cubic Dresselhaus contribution. Equation (2) results from sequential perturbative expansions up to third order in k and to first order with respect to the inverse splitting $\Delta_{\mathrm{HL}}^{-1}$ and to E_z imposed on the crystal. The identification of enhanced spin relaxation times in this work is closely connected with broken axial symmetry, since here a conserved quantity related to the spin degree of freedom can only be constructed in the presence of terms with both two- and threefold rotational symmetry in the extrinsic and the intrinsic SOI. Although our findings suggest that obtaining an exact PSH symmetry may be limited by the parameters of realistic systems, an approximate symmetry in the leading-order Fourier components of Ω_{2DHG} causes a weakly perturbed crossover from WAL to WL, similar to electronic systems with cubic intrinsic SOI [11].

The effect of the spin symmetry on the magnetoconductance G can be analyzed by organizing the transmission entering the Landauer-Büttiker framework [24, 25],

$$\frac{h}{e^2} G = \left(\sum_{n,m;\sigma=\sigma'} + \sum_{n,m;\sigma\neq\sigma'} \right) |t_{n\sigma,m\sigma'}|^2 =: T_{\mathrm{D}} + T_{\mathrm{OD}}, \tag{6}$$

according to their spin quantum numbers σ, σ' in terms of diagonal spin-preserving channels T_{D} and a spin off-diagonal contribution T_{OD}. Here, $\sigma, \sigma' = \pm 1$ refer to an arbitrary basis defined in the ballistic leads of a two-terminal device representing our numerical model, while n, m are integers that define the transverse channel of the in- and outgoing states due to a hard-wall confinement of the leads. The lead wavefunctions $|\phi_{n,\sigma}\rangle$ and $|\phi_{m,\sigma'}\rangle$ enter into the Fisher-Lee relation for the amplitudes

$t_{n\sigma,m\sigma'} \propto \int_{\partial\mathrm{Leads}} \mathrm{d}^2\mathrm{r} \langle \phi_{n,\sigma}| \mathrm{y}_1 \rangle \langle \mathrm{y}_1| \mathrm{G_R} |\mathrm{y}_2 \rangle \langle \mathrm{y}_2 |\phi_{m,\sigma'}\rangle$, where the integration is taken over the lead cross sections [26]. $\mathrm{G_R} = (E_{\mathrm{F}} - \mathrm{H} + 0_+)^{-1}$ is the Green's function of the scattering region at fixed Fermi energy E_{F}.

Knap et al. [9] found in n-type systems particular relations between extrinsic and intrinsic SOI magnitude, for which the Cooperon becomes separable and a WL signal rather than WAL is observed. In terms of the structure provided by Eq. (6), T_{OD} vanishes in this case and correspondingly spin scattering is absent even in transport in disordered systems. This is equivalent to the observation that the system displays an exact, disorder independent symmetry [2, 3], which allows for a decomposition within the corresponding constant eigenbasis $\{|\chi_\sigma\rangle\}$ into $\mathbf{\Omega}\cdot\boldsymbol{\sigma} = \sum_{\sigma=\pm 1} E_\sigma(\mathbf{\Omega}) |\chi_\sigma\rangle \langle\chi_\sigma|$. Hence, when taking the spin trace in Eq. (6) in the basis $\{|\chi_\sigma\rangle = (1, \sigma \exp[\pm i\pi/4])^\dagger\}$, corresponding to the existence of the conserved quantity $\Sigma_\pm = \sigma_x \pm \sigma_y$ or, equivalently, fixed in-plane spin orientation along $\theta = \pm\pi/4$, one finds that $T_{\mathrm{OD}} \propto \sum_{\sigma\neq\sigma'} |\langle\chi_\sigma|\chi_{\sigma'}\rangle|^2 = \sum_{\sigma\neq\sigma'} \delta_{\sigma,\sigma'}$ is supressed and T_{D} decomposes into two independent channels which trivially display WL [9].

In the hole model (2) we find the analogue to the electronic PSH symmetry if the system parameters fulfill $\lambda_{\mathrm{R}}/\lambda_{\mathrm{D}} = \pm 1$ and $\bar{\gamma} = -\delta$, i.e., $\gamma_3 = 0$. In these two cases the direction of Ω_{2DHG} is fixed independently of the momentum, more precisely by $\mathbf{\Omega}_{\mathrm{2DHG}} \propto [-k_{\mathrm{F}}^2(k_x \pm k_y) \pm 3k_xk_y(k_x \pm k_y) - k_x^3 \mp k_y^3](\hat{\boldsymbol{x}} \pm \hat{\boldsymbol{y}})$. We illustrate these cases in Fig. 1, where the effective spin-orbit field Ω_{2DHG} is oriented along a fixed direction for both spin-split subbands [34]. By engineering the quantum well width and choosing the electrical gate field appropriately, a regime of enhanced spin lifetime should be accessible in hole gases. In realistic material systems it is possible to influence the effective values of γ_3 [35]. In particular at $\lambda_{\mathrm{R}}/\lambda_{\mathrm{D}} = -1$ and $\gamma_3 = 0$, as investigated in Fig. 2, the symmetric situation is obtained.

The symmetry condition becomes apparent in the magnetoconductance of disordered 2DHG systems, as illustrated in Fig. 2. There we show results of the numerically calculated disorder averaged transmission, Eq. (6), for finite cubic intrinsic SOI λ_{D} as a function of the extrinsic SOI λ_{R}, respectively the parameter $\eta = \lambda_{\mathrm{R}}/\lambda_{\mathrm{D}}$, setting $\gamma_3 = 0$. Representative examples of the conductance correction traces are shown in Fig. 2(a), which display typical WAL and WL lineshapes as a function of magnetic flux ϕ from a homogeneous magnetic field perpendicular to the 2DHG plane. Considering the dependence on $\eta = \lambda_{\mathrm{R}}/\lambda_{\mathrm{D}}$, we find pronounced signatures of WAL if η is far from -1. When η approaches the value of -1, a crossover from WAL to WL occurs as indicated by a maximum negative conductance correction, in agreement with the symmetry argument. In Fig. 2(b) our results are summarized in terms of the conductance at maximum magnetic flux $\langle T(\phi_{\mathrm{max}})\rangle$ subtracted from the correction at zero flux $\langle T(0)\rangle$ plotted as a function of η, where we
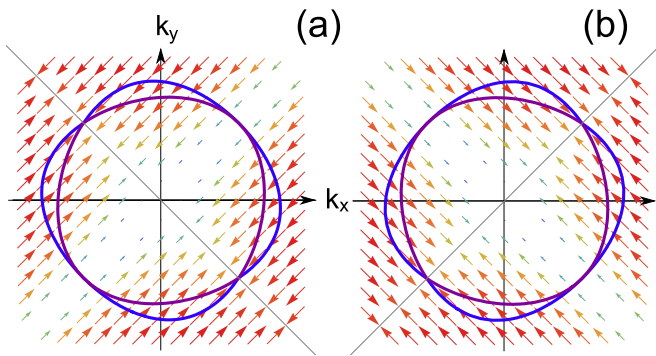
Figure 1: (Color online) Fermi surface for the different spin directions obtained from Eq. (1) (violet and blue contours) and the corresponding direction of the effective spin-orbit field, $\mathbf{\Omega}_{\text{2DHG}}$, illustrated by arrows. The SOI parameters establish a persistent spin helix for holes with uniaxial spin orientation corresponding to $\lambda_{\text{R}}/\lambda_{\text{D}} = +1$ (a) or $\lambda_{\text{R}}/\lambda_{\text{D}} = -1$ (b). In both cases the Luttinger-Kohn parameters are $\bar{\gamma} = -\delta$, i.e., $\gamma_3 = 0$.
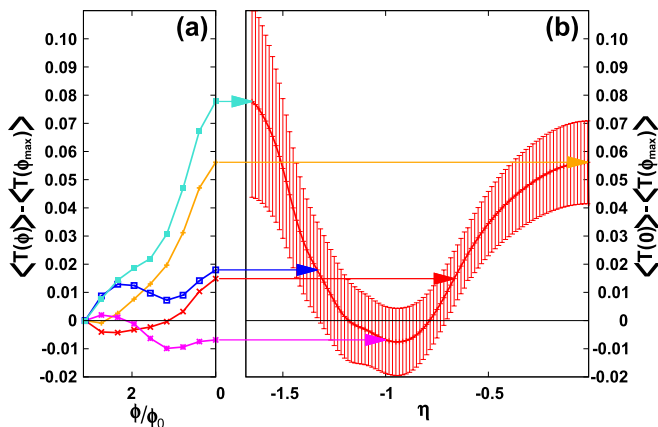

Figure 2: (Color online) Signatures of spin-preserving symmetries in weak localization of a two-dimensional hole gas. (a) Disorder-averaged magneto conductance correction $\langle T(\phi) \rangle - \langle T(\phi_{\text{max}}) \rangle$ as a function of flux ϕ (in units of $\phi_0 = h/e$; $\phi_{\text{max}}/\phi_0 = 3.1$) for spin-orbit coupling ratios $\eta = \lambda_{\text{R}}/\lambda_{\text{D}} = -1.65, -0.017, -1.33, -0.67, -1$ (from top to bottom).
(b) Conductance correction $\langle T(0) \rangle - \langle T(\phi_{\text{max}}) \rangle$ as a function of η. Negative magneto conductance reflects suppression of spin relaxation close to $\eta = -1$. System parameters used in (a) and (b): Disorder average over 1000 impurity configurations for a scattering region of aspect ratio (length to width W) 200:80 unit cells with periodic boundary conditions in transverse direction. Quantum transmission computed for $k_{\text{F}}W/\pi = 13$ hole states per spin supported in the leads, elastic mean free path $l = 0.04W$, $\gamma_3 = 0$, and fixed Dresselhaus spin precession length $k_{\text{D}}W \approx 1$, defined below Eq. (8).

chose $\phi_{\text{max}} = 3.1\phi_0$. The results show that the parameter regime where a PSH type symmetry occurs is characterized by a negative conductance correction, i.e., by a WL signature.

Our analysis above is confirmed within a diagrammatic perturbative treatment by exact diagonalization

of the Cooperon $\hat{C}(\mathbf{Q})$ in the framework of the effective model (1). For this purpose the scheme presented in Refs. [27, 28] for electrons is generalized to holes. The diagrammatic approach is justified since we assume to be in the diffusive regime, $E_{\text{F}}\tau \gg 1$, with elastic scattering time τ. Since we consider the spin $\pm 3/2$ subspace, one is left with [29]

$$\hat{C}(\mathbf{Q}) = \frac{\hbar}{D_h \left(\hbar\mathbf{Q} + \frac{2}{3}m_0 \langle \hat{a} \rangle \cdot \mathbf{S} \right)^2 + H_c}, \qquad (7)$$

where $D_h = \tau v_{\text{F}}^2/2$ is the diffusion constant, $\mathbf{Q} = \mathbf{k} + \mathbf{k}'$ the Cooperon momentum composed of momenta of the retarded and advanced propagators with spins $3/2\hbar\boldsymbol{\sigma}$ and $3/2\hbar\boldsymbol{\sigma}'$, giving rise to $\mathbf{S} = 3/2\hbar(\boldsymbol{\sigma} + \boldsymbol{\sigma}')$. In Eq. (7) the average over all directions of the velocity $\mathbf{v}_{\text{F}}$ on the Fermi surface is denoted by $\langle \ldots \rangle$, and $\hat{a}$ is defined via the relation $\boldsymbol{\sigma} \cdot \mathbf{\Omega}_{\text{2DHG}} = \mathbf{k} \cdot (\hat{a} \cdot \boldsymbol{\sigma})$ describing the Rashba and Dresselhaus SOI. H_c is a $\mathbf{Q}$-independent term which generally leads to spin relaxation. However it can be shown that one of the gaps of the eigenmodes in the triplet sector of the Cooperon vanishes if the aforementioned symmetries are present. Since the Cooperon gaps can be interpreted as spin-relaxation rates [27, 28], this supports the numerical findings of persistent spin states.

The numerical setups on which our simulations are based are disordered hole systems connected to two terminals, represented by ballistic semi-infinite leads without SOI. The latter is switched on and off adiabatically over one fifth of the total length of a rectangular scattering region to which the leads are connected. We use an average over an Anderson-like uniformly distributed random-box potential V_{dis} to simulate disorder. The perpendicular magnetic field is included by means of the Peierls substitution. The Hamiltonian is then discretized on a tight-binding grid in position space and the transmission amplitudes are obtained by an optimized recursive Green's function algorithm [30]. Since we are interested in modeling bulk transport, we implemented periodic boundary conditions in the transverse direction to minimize effects from the boundaries.

Apart from considering the indirect influence of the PSH symmetry on the WL-WAL transition, it seems natural to search for a manifestation of a symmetry in T_{D}, Eq. (6), since its effects could be determined by magnetic polarization of the leads, allowing for spin transistor operation even in the presence of disorder [2]. Numerically we can confirm the validity of the latter approach by calculating the normalized quantity $T_{\text{D}}/(T_{\text{D}} + T_{\text{OD}})$ as a function $\eta = \lambda_{\text{R}}/\lambda_{\text{D}}$, as shown in Fig. 3. We identify a pronounced transmission maximum at $\eta = 1$ in the basis corresponding to the $+\pi/4$ spin orientation even in situations where the exact PSH-type symmetry is not realized. In the given example we chose the Luttinger-Kohn parameters $\gamma_2 = 1$ and $\gamma_3 = 0.25$ which correspond to such a nonideal setup. For parameters far from $\eta = 1$
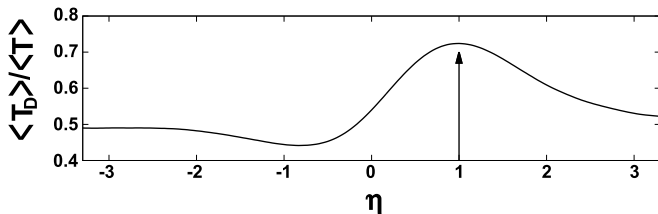
Figure 3: Ratio of disorder averaged diagonal transmission over total transmission $\langle T_\mathrm{D}\rangle / \langle T\rangle = \langle T_\mathrm{D}\rangle / \langle T_\mathrm{D} + T_\mathrm{OD}\rangle$ as a function of η for a scattering region with 150:80 aspect ratio for fixed Dresselhaus spin precession length $k_\mathrm{D}^{-1} = 1.3\, W$ and Luttinger-Kohn parameters $\gamma_2 = 1$ and $\gamma_3 = 0.25$ for which no exact spin-preserving symmetry can be established. The peak of $\langle T_\mathrm{D}\rangle / \langle T\rangle$ at $\eta = 1$, coincides with the maximum of the diabatic transition probability of Eq. (8) (indicated by the arrow). Average Transmission shown includes 1000 disorder configurations.

the spin transmission is equally distributed among the diagonal and off-diagonal channels.

When $|\eta|$ approaches 1, T_D formally corresponds to the probability of diabatic Landau-Zener transitions between instantaneous eigenstates $|\pm\boldsymbol{\Omega}\rangle = (1, \pm\exp[-i\arctan(\Omega_y/\Omega_x)])^\dagger$ of the spin-orbit contribution (2). The momentum direction is changed by disorder scattering such that the spin evolution is subject to inhomogeneties of the effective spin-orbit field $\boldsymbol{\Omega}$.

At the minima of the anisotropic spin splitting $2\,|E_\sigma(\boldsymbol{\Omega})|$, this induces transitions of the type $|\pm\boldsymbol{\Omega}\rangle \to |\mp\boldsymbol{\Omega}\rangle$ with Landau-Zener transition probability P_D [31, 32]. These transitions enhance the value of T_D while completely suppressing T_OD for $P_\mathrm{D} = 1$. The spinors $\{|\chi_\sigma\rangle\}$ underlying Eq. (6) coincide with the diabatic superposition of the states $|\pm\boldsymbol{\Omega}\rangle$. The latter can be checked by considering $\langle\chi_\sigma|\boldsymbol{\Omega}\cdot\boldsymbol{\sigma}|\chi_\sigma\rangle$. Within the HH model (2) the diabatic basis coincides with that of the PSH eigenstates $\{|\chi_\sigma\rangle\}$ of a 2DEG [2]. For p-type systems we find a probability [36]

$$\ln(P_\mathrm{D})_\mathrm{2DHG} = \zeta l |k_D|\, |\bar{\gamma} + \delta|\, (1 - |\eta|)^2, \qquad (8)$$

with the elastic mean free path l and a correction factor ζ entering together with the transport time τ into the rate of change in angle θ in the relation $\delta\theta = \pi/2\delta t/(\tau\zeta)$. Equation (8) is derived under the assumption that $\bar{\gamma} \neq -\delta$. Although the expression for the Landau Zener transition probability predicts a clear maximum at $|\eta| = 1$, Equation (8) does not cover the description of T_D for parameters where the PSH symmetry is established. It is nevertheless applicable to realistic material parameters when $\gamma_3 \neq 0$ and consequently $\bar{\gamma} \neq \delta$, which is verified by a numerical transport analysis.

The analyis of T_D can be applied to electronic systems as well, with an effective spin-orbit field,

$$\boldsymbol{\Omega}_\mathrm{2DEG} = \alpha\boldsymbol{k}\times\hat{\boldsymbol{z}} + \beta\left(k_x\hat{\boldsymbol{x}} - k_y\hat{\boldsymbol{y}}\right) + \gamma\left(-k_x k_y^2\hat{\boldsymbol{x}} + k_y k_x^2\hat{\boldsymbol{y}}\right),$$
$$(9)$$

for transport along the [100] direction in a 2DEG grown in [001] direction and with $\langle k_z^2\rangle\gamma = \beta$ [9]. In systems described by this model the corresponding Landau-Zener transition probability is given by

$$\ln(P_\mathrm{D})_\mathrm{2DEG} = \zeta l |k_\beta|\, (\Gamma_\beta/2 - 1 \pm \eta)^2, \qquad (10)$$

with the Dresselhaus spin precession length $k_\beta^{-1} = \left(m_\mathrm{eff}\beta/\hbar^2\right)^{-1}$, ratio of cubic and linear SOI $\Gamma_\beta = k_\mathrm{F}^2\gamma/\beta$ and correction factor ζ as it appears in Eq. (8). This model has been verified by numerical calculations which are beyond the scope of this work.

In both p- and n-type systems, the signatures in T_D are robust against disorder. Therefore as an experimental approach to analyzing spin relaxation lengths in transport within HH systems, a detection of the PSH signature in the longitudinal conductance of a spin-polarized current is favorable. The mechanism responsible for the peaks in T_D the momentum space analogue to the effect of a spatially inhomogeneous helix-type Zeeman term on the spin conductance in dilute magnetic semiconductors [33]. An alternative measurement method for further investigation of the HH PSH is represented by magneto-optical Kerr rotation techniques, which recently allowed to map the spin topology in electronic systems [5].

————————

[1] I. Žutić, J. Fabian, and S. Das Sarma, Rev. Mod. Phys. **76**, 323 (2004).
[2] J. Schliemann, J. C. Egues, and D. Loss, Phys. Rev. Lett. **90**, 146801 (2003).
[3] B. A. Bernevig, J. Orenstein, and S.-C. Zhang, Phys. Rev. Lett. **97**, 236601 (2006).
[4] J. D. Koralek, C. P. Weber, J. Orenstein, B. A. Bernevig, S.-C. Zhang, S. Mack, and D. D. Awschalom, Nature **458**, 610 (2009).
[5] M. P. Walser, C. Reichl, W. Wegscheider, and G. Salis, Nat. Phys. **8**, 757 (2012).
[6] E. I. Rashba, Sov. Phys. Solid State (1960).
[7] G. Dresselhaus, Phys. Rev. **100**, 580 (1955).
[8] F. G. Pikus and G. E. Pikus, Phys. Rev. B **51**, 16928 (1995).
[9] W. Knap, C. Skierbiszewski, A. Zduniak, E. Litwin-Staszewska, D. Bertho, F. Kobbi, J. L. Robert, G. E. Pikus, F. G. Pikus, S. V. Iordanskii, et al., Phys. Rev. B **53**, 3912 (1996).
[10] S. Hikami, A. I. Larkin, and Y. Nagaoka, Prog. of Theo. Phys. **63**, 707 (1980).
[11] M. Kohda, V. Lechner, Y. Kunihashi, T. Dollinger, P. Olbrich, C. Schönhuber, I. Caspers, V. V. Bel'kov, L. E. Golub, D. Weiss, et al., Phys. Rev. B **86**, 081306 (2012).
[12] M. Glazov and L. Golub, Semiconductors **40**, 1209 (2006).

[13] M. C. Lüffe, J. Kailasvuori, and T. S. Nunner, Phys. Rev. B **84**, 075326 (2011).

[14] N. Averkiev, L. Golub, and G. Pikus, Solid State Communications **107**, 757 (1998).

[15] I. Garate, J. Sinova, T. Jungwirth, and A. H. MacDonald, Phys. Rev. B **79**, 155207 (2009).

[16] V. Krueckl, M. Wimmer, i. d. I. Adagideli, J. Kuipers, and K. Richter, Phys. Rev. Lett. **106**, 146801 (2011).

[17] J. M. Luttinger and W. Kohn, Phys. Rev. **97**, 869 (1955).

[18] R. Winkler, H. Noh, E. Tutuc, and M. Shayegan, Phys. Rev. B **65**, 155303 (2002).

[19] D. V. Bulaev and D. Loss, Phys. Rev. Lett. **95**, 076805 (2005).

[20] R. Winkler, *Spin-Orbit Coupling Effects in Two-Dim-ensional Electron and Hole Systems* (Springer Berlin, 2003).

[21] N. O. Lipari and A. Baldereschi, Phys. Rev. Lett. **25**, 1660 (1970).

[22] X. Bi, P. He, E. Hankiewicz, R. Winkler, G. Vignale, and D. Culcer.

[23] A. Scholz, T. Dollinger, P. Wenk, K. Richter, and J. Schliemann, Phys. Rev. B **87**, 085321 (2013).

[24] R. Landauer, IBM J. Res. Develop. **1**, 223 (1957).

[25] M. Büttiker, Y. Imry, R. Landauer, and S. Pinhas, Phys. Rev. B **31**, 6207 (1985).

[26] D. S. Fisher and P. A. Lee, Phys. Rev. B **23**, 6851 (1981).

[27] S. Kettemann, Phys. Rev. Lett. **98**, 176808 (2007).

[28] P. Wenk and S. Kettemann, Phys. Rev. B **81**, 125309 (2010).

[29] P. Wenk (2012).

[30] M. Wimmer and K. Richter, J. Comput. Phys. **228**, 8548 (2009).

[31] L. Landau, Physics of the Soviet Union **2**, 46 (1932).

[32] C. Zener, Proc. R. Soc. Lon. A **137**, 696 (1932).

[33] C. Betthausen, T. Dollinger, H. Saarikoski, V. Kolkovsky, G. Karczewski, T. Wojtowicz, K. Richter, and D. Weiss, Science **337**, 324 (2012).

[34] The structure of Eq. (2) implies an additional symmetry for $\bar{\eta} = 0$, which is however outside the range of validity since it corresponds to $\gamma_2 = 0$ and thereby a breakdown of perturbation theory.

[35] See Table C.9 in Ref. [20]

[36] $P_\mathrm{D} = \exp\left[-2\pi\epsilon_{12}^2/\left(\hbar\left|\partial_t\left(\epsilon_1(t) - \epsilon_2(t)\right)\right|\right)\right]$ within Zener's simplified model [32]. The numerical value can be calculated from the knowledge of the minimal spin splitting, $2\epsilon_{12}$, in the corresponding directions $\theta := \arctan(k_y/k_x)$ and the slope of the splitting, $\epsilon_1(t) - \epsilon_2(t)$, between the fully diabatically coupled basis states.